Interactions between a heavy particle, air, and a layer of liquid 🅕

E. M. Jolley ✉ ; F. T. Smith

Check for updates

View Online   Export Citation   CrossMark

Articles You May Be Interested In

Pre-impact dynamics of a droplet impinging on a deformable surface
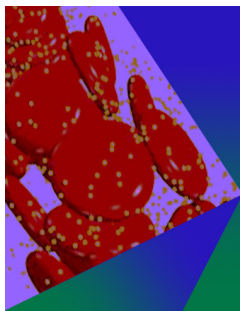
Physics of Fluids (September 2021)

Collisions, rebounds and skimming

AIP Conference Proceedings (October 2013)

A radio-frequency Bose–Einstein condensate magnetometer

Appl. Phys. Lett. (April 2022)

Interactions between a heavy particle, air, and a layer of liquid 🅕

E. M. Jolley[a] 🅧 and F. T. Smith

AFFILIATIONS

Department of Mathematics, University College London, London WC1E 6BT, United Kingdom

[a]Author to whom correspondence should be addressed: ellen.jolley.18@ucl.ac.uk

ABSTRACT

As an aircraft flies through cloud at temperatures below freezing, it encounters ice particles and supercooled droplets, which results in the accretion of ice onto its surfaces and hence deformation of its aerodynamic shape. This can, in worst cases, cause series accidents. Here, we focus on tackling the common situation where there is a thin layer of water on the aircraft surface and the particles are similarly thin such as to be able to interact with the water layer. Three-way interaction occurs between air, water, and body motion: under suitable assumptions (including that the Reynolds and Froude numbers are large, and that the body is much denser than the air), the model allows the shape of the layer interface and pressure profile beneath the body to be calculated for a given body position. Simultaneously, this in turn allows the forces on the body to be calculated and hence the motion of the particle to be computed in full. The result is a wide range of possible motions of the particle, including both "sink" cases (the particle enters the water and becomes submerged) and "skim" cases (where the particle is launched back off the surface of the water following contact). The latter cases have analogy with traditional "stone skimming/skipping" games. Repeated skims and significant wakes are accommodated rationally.

I. INTRODUCTION

We consider a rigid body (particle, object) moving under the pressure forces of a high-Reynolds number air flow above a wall coated in a layer of fluid (liquid, say) whose density is greater than that of air. The dynamics are fully coupled, so the movement of the body affects the surrounding flow and liquid layer position, and vice versa. In the case that the body impacts with the layer, we also analyze subsequent interactions between the body, the air, and the liquid layer, including both "skimming" and "sinking" behavior. High Reynolds numbers are of interest because of many applications. The application most in mind is aircraft icing, wherein ice particles may adhere to the surfaces of aircraft and degrade performance (Gent *et al.*, 2000; Purvis and Smith, 2016; Janjua *et al.*, 2018). In this context, aircraft may become coated in a thin layer of water after flying through clouds, and the interactions of incoming ice with this layer then affect the formation of further ice. The aircraft-icing application is a prime motivation for the present study where, in contrast to previous studies, we now seek to incorporate body–air–liquid interplay.

The initial problem of a body moving in an air flow above a layer is related to the air–body interaction scenario studied in Jolley and Smith (2022) and Jolley *et al.* (2021). In that scenario, a body, assumed to be much more dense than the surrounding air, moves under the effects of an incoming boundary layer flow in the vicinity of a wall. This system displays a wide variety of behaviors, and in particular, the body may "fly away," i.e., the body escapes from the wall at large times and does not return. The various behaviors can occur in the present system also, with fly-away effectively unchanged from the analysis in the above papers (since as the body becomes very distant from the liquid layer its influence becomes negligible). In this paper, we therefore focus on solutions where the body moves toward the liquid layer such as to eventually impact. In the absence of air, this is known as the water entry problem. Water entry problems have been much studied over the years, going back to Von Kármán (1929); Wagner (1932). In these works, it is typical that a jet forms along the perimeter of the impacting body. This was first hypothesized by Wagner (1932) and developed using matched asymptotic expansions in, for example, Cointe and Armand (1987), Howison *et al.* (1991) in the context of deep water-entry, and by Korobkin (1995) for shallow water. Howison *et al.* (2004) considered the structure of the jet in the context of oblique impacts, which is most relevant for skimming problems. However, the vertical motion of the body in their paper is prescribed and so there can be no analysis of the rebound.

Stone skimming or skipping will be familiar to many readers from a childhood (and others'!) game, known (among other names) as *ducks and drakes*. Recent media attention (Sample, 2023; Pinkstone, 2023) given to the paper by Palmer and Smith (2023) demonstrates the significant popular interest in the topic. The paper by Tuck and Dixon (1989) is of particular relevance to the present study, as we make use of the momentum jump condition at the jet root derived in that paper. The model used in this paper, including the use of the Tuck and Dixon criterion, is related to the model used by Hicks and Smith (2011), among others (Liu and Smith, 2014; 2021; Palmer and Smith, 2020; 2022; 2023). Other recent studies of stone skimming include Tang *et al.* (2021); Li *et al.* (2021). In this two-dimensional model, the body and water layer are assumed thin, air effects are neglected, and the body is taken to have a sharp trailing edge such that during impact the water flow always detaches there (the effect of a smooth trailing edge is considered in Liu and Smith, 2021). The model used in the current work differs from the models just mentioned in the inclusion of air dynamics throughout the particle motion, bringing together the body–air interaction problem considered in Jolley and Smith (2022) with the interactions with the liquid layer, and allowing modeling of repeat skims among other phenomena. Here, the density ratio between the air and the liquid layer is assumed to be of order unity in general, and the water case is studied by taking the density ratio to be large—hence, generally we avoid referring to the layer as a "water layer" in this paper. Note that the generality of the model means that the layer could be a gas instead of a liquid.

Our main focus in this work is to allow rationally for pre- and post-impact interactions between air, liquid and body motion, including a moving contact point in the post-impact situation. The work is also to admit fully nonlinear skimming and/or sinking of the body, in contrast with many studies (Hicks and Smith, 2011; Liu and Smith, 2014; 2021; Palmer and Smith, 2020; 2022; 2023).

The paper begins by outlining the body/air/liquid layer interaction model for the pre-impact stage (when the body is not in contact with the layer) in Sec. II. Asymptotic analysis of impacts with the layer are then given first for the general case in Sec. III and then for the case of large density ratio between the air and the liquid (i.e., approaching the case of a water layer) in Sec. IV. Then in Sec. V, the model for the post-impact motion (i.e., during skim) of the body is described and numerical results pairing the solutions of the two problems showing repeat skims are presented. In Sec. VI, the possibility of the body coming into contact with the wall beneath the layer is considered and asymptotically described. In Sec. VII, the inclusion of the gravity effects on the body motion is investigated and a further set of numerical results presented. Finally, Sec. VIII discusses implications of the work and future extensions to be considered.

II. BODY/AIR/LIQUID LAYER INTERACTION MODEL

A diagram showing the problem setup is shown in Fig. 1. The non-dimensionalization here is based on the typical oncoming air velocity, the air density, and the length of the thin body. The work is in terms of body-centered coordinates such that effectively the velocity u_c in the figure is subtracted from u^a, u^w. The body moves in an air or other gas flow above a surface coated in a layer of liquid with density ρ_w, with $\rho_w > \rho_a$ where ρ_a is the air density. We define the density ratio $E = \rho_w/\rho_a > 1$. Note again that, although for the industrial application we are interested in a water layer, this liquid is not in
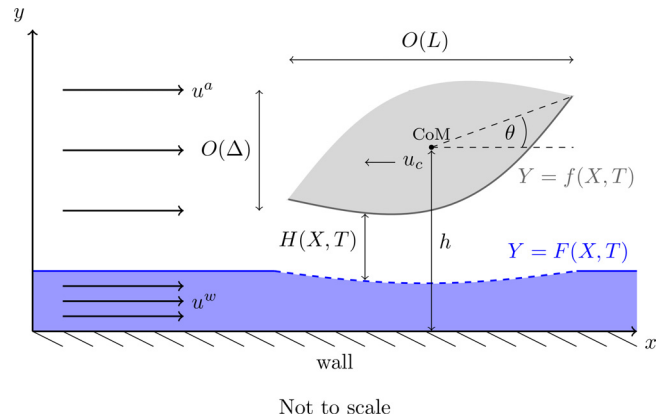

FIG. 1. A diagram showing the non-dimensional problem setup. A thin body translates with velocity u_c through a gas (e.g., air) near a wall coated in a layer of liquid (e.g., water). The height of the body's center of mass is h, and the angle its chord line makes with the x-axis is θ. The incoming velocity profile is $u = u^a$ in the air and $u = u^w$ in the liquid. Note the liquid could instead be another gas. The shape of the dashed portion of the liquid layer interface is to be found.

general assumed to be water; instead the water case will be investigated by taking a specific large value of the density ratio E afterward. We thus have three-way coupling wherein the body motion, the air pressure and the height of the liquid layer all interact with each other.

We assume that the body is small and thinner than it is long, of width Δ and length L where $\Delta \ll L$. We also assume that both the liquid layer height and the initial air gap between the body and the layer are $O(\Delta)$. In aircraft icing applications, we anticipate flows with high Reynolds, Froude and Weber numbers, meaning as discussed in Purvis and Smith (2016) that the effects of viscosity, gravity and surface tension are nominally negligible (although the effects of gravity are considered in Sec. VII). See discussion of flow separation effects in Smith and Ellis (2010); Jolley *et al.* (2021); Smith and Servini (2019). The body is translating in the upstream direction, but we work in its rest frame so this effectively means positive tangential velocity at the wall. We consider bodies whose density is much greater than that of the surrounding fluid (as for ice in air). We take the incoming flow (i.e., upstream of the body) both in the air and in the liquid layer as uniform. Due to the assumption that the body, liquid layer, and the air gap between them are significantly thinner than they are wide, we can neglect vertical variations in the problem, so in our re-scaled coordinates the non-dimensional governing equation for the air is

$$\varepsilon u_T + u u_X = -p_X, \quad p_Y = 0, \tag{1}$$

where X is the horizontal Cartesian coordinate scaled such that $X = 0$ at the leading edge of the body and $X = 1$ at the trailing edge, and Y is the vertical coordinate scaled by Δ such that the layer height is at $Y = 1$ in the absence of effects from the body. Also, T is a time coordinate scaled according to the body motion (more detail below), u is the horizontal velocity in the air flow, p is the air pressure, and $\varepsilon = (L/\Delta)(\rho_a/\rho_B)^{1/2}$ (for body density ρ_B) is a constant arising from the time scaling which we assume to be small based on the small density of air compared to the body density. Hence the air flow is modeled as steady. This allows Bernoulli's theorem to be applied. We assume the air flow is incoming with uniform velocity $u = 1$, and thus,

$$\frac{1}{2}u^2 + p = \frac{1}{2}, \tag{2}$$

holds. There is an Euler region just upstream of the leading edge of the body, where the incoming flow adapts to the presence of the body (Jones and Smith, 2003; Smith and Servini, 2019). Since this region is also steady, Eq. (2) holds throughout the air flow, subject to replacing u by the flow speed within the Euler region.

The body motion is governed solely by the pressure force under the body (which is an order of magnitude greater than that above the body). Hence

$$Mh_{TT} = \int_0^1 p\, dX, \quad I\theta_{TT} = \int_0^1 (X - \beta)p\, dX, \tag{3}$$

where h is the Y-coordinate of the center of mass, β is its X-coordinate, θ is the angle of the body chord to the X-axis, $M = \hat{M}/(\rho_B L\Delta)$ and $I = \hat{I}/(\rho_B L^3\Delta)$ are the non-dimensional mass and moment of inertia, respectively (compared to dimensional equivalents $\hat{M}$ and $\hat{I}$). The balance of scales in Eq. (3) gives the body motion timescale as $\Delta(\rho_B/\rho_a)^{1/2}$, which leads to the value of ε given in the previous paragraph. The underbody curve is given by

$$Y = f(X, T) = f_u(X) + h(T) + (X - \beta)\theta(T). \tag{4}$$

Equations (1) and (3) define the body–air interaction problem, which displays an intriguing variety of solutions even in the absence of a liquid layer, including several distinct cases of fly-away solutions where the body height tends to infinity as time tends to infinity. The body–air system is discussed at length in Jolley and Smith (2022) and Jolley et al. (2021).

The Weber number is large, to repeat, and so we do not include surface tension effects. Since there is no vertical variation, this then dictates that the pressure in the liquid layer is everywhere equal to that in the air (a consequence of applying the dynamic boundary condition at the interface). We model the layer flow as quasi-steady, obeying an analogous equation to Eq. (1) with allowance for the different densities; thus

$$\varepsilon u_T + uu_X = -\frac{1}{E}p_X \tag{5}$$

leading to

$$\frac{1}{2}u^2 + \frac{1}{E}p = \frac{1}{2}, \tag{6}$$

when ε is small as assumed. The above requires the assumption that the density of the liquid in the layer is much less than the density of the body [specifically, $\rho_w/\rho_B \ll (\Delta/L)^2$]. This is false for ice in water, where the density ratio ρ_w/ρ_B is approximately unity (a case which is addressed in the final discussion of the paper), however it applies for either a denser body or a lighter fluid, and the ice in water case can still be studied to some extent in the limit of large ρ_w as considered in Sec. IV. The unknown interfacial curve is given by $Y = F(X, T)$, and we denote the unknown air gap width by $Y = H(X, T) = f(X, T) - F(X, T)$. Assuming $E = O(1)$ in general, Bernoulli's theorem combined with mass conservation of uH in the air and of uF in the liquid yields the flow equations as follows:

$$p + \frac{1}{2}\frac{H(1, T)^2}{H(X, T)^2} = \frac{1}{2} \quad \text{(in air)}, \tag{7}$$

$$\frac{p}{E} + \frac{1}{2}\frac{F(1, T)^2}{F(X, T)^2} = \frac{1}{2} \quad \text{(in liquid)}. \tag{8}$$

The Kutta condition applying at the trailing edge of the body forces the pressure to be zero there and consequently the height of the layer there is fixed at $F(1, T) = 1$, by virtue of the Bernoulli and mass-conservation properties holding all the way from just upstream of the Euler zone to the trailing edge and p being zero in both locations. Enforcing this requirement and equating the pressures in Eqs. (7) and (8) leads to a quartic relation between the body position and layer height, namely,

$$((1 - E)F(X, T)^2 + E)H(X, T)^2 = H(1, T)^2 F(X, T)^2. \tag{9}$$

This enables both the layer height and pressure to be found for a given body position, and thus for the system of integro-ordinary differential equations in Eq. (3) to be integrated numerically.

III. ANALYSIS OF IMPACT ONTO THE LIQUID LAYER

The problem given by Eq. (3) to Eq. (9) displays both solutions where the body lifts off from its initial position and solutions where it approaches the liquid layer. In the former category, the presence of the layer as expected has increasingly small effect as the body departs. Therefore, these solutions are effectively unchanged from those in the body–air system, which are discussed at length in Jolley and Smith (2022). Thus, we focus on solutions where the body approaches and subsequently impacts on the layer, which we analyze here for general density ratio, i.e., $E = O(1)$, and in Sec. IV for large density ratio, $E \gg 1$.

Inspecting the quartic Eq. (9), we see that for the body to impact on the layer, i.e., $H(X, T) = 0$ for some X, either $H(1, T) = 0$ or $F(X, T) = 0$. The former corresponds to the trailing edge of the body being in contact with the layer, while the latter corresponds to both the body and the free surface touching the wall at the same point. We focus for now on the former option, but the latter is discussed in the Appendix. Assuming then that the trailing edge has impacted (say at time T_0), as in Figs. 2–5, we see for $0 \le X < 1$ there are two positive roots,

$$F(X, T_0) = f(X, T_0) \quad \text{and} \quad F(X, T_0) = 1/\alpha, \quad \text{where } \alpha = \sqrt{1 - 1/E}. \tag{10}$$

The first of these roots corresponds to impact (where the gap between the body and the free surface tends to zero), while the second is a constant level which approaches 1 in the limit of large E. We also require $F(X, T) \le 1/\alpha$ throughout the motion [or else the right-hand side of Eq. (9) is negative], hence impact is only possible at a given X if f moves below height $1/\alpha$, and we can state that the liquid surface has

$$F(X, T_0) = \min[f(X, T_0), 1/\alpha] \tag{11}$$

at impact. This can be seen in the numerical results displayed in Figs. 2 and 3, for $E = 2$. In Fig. 2, the body angle is sufficiently negative to allow the body to impact at the trailing edge while remaining above the $1/\alpha$ level (i.e., $\sqrt{2}$ here) at the leading edge: see the curved interface. In Fig. 3, the body angle is positive, meaning it impacts along the full length of the underbody.

Taking the gap width $H(X, T)$ to be small for some values of X, and using the feature that the trailing edge height $F(1, T)$ remains
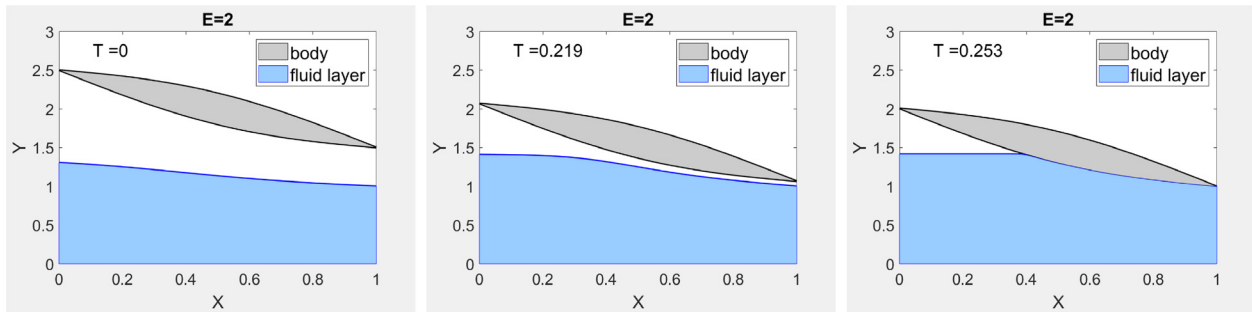
FIG. 2. The body motion and layer reaction at three points in time for a density ratio $E = 2$ and an initially negative body angle, $\theta(0) = -1$. In the final impact, the layer is either in contact with the body or at the constant level $\sqrt{2}$.
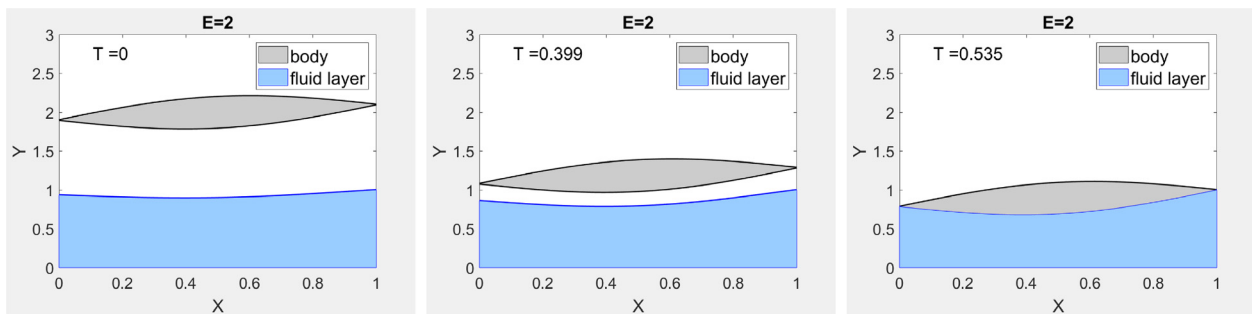

FIG. 3. The body motion and layer reaction at three points in time for a density ratio $E = 2$ and an initially positive body angle, $\theta(0) = 0.2$. In the final impact, the layer is everywhere in contact with the body.
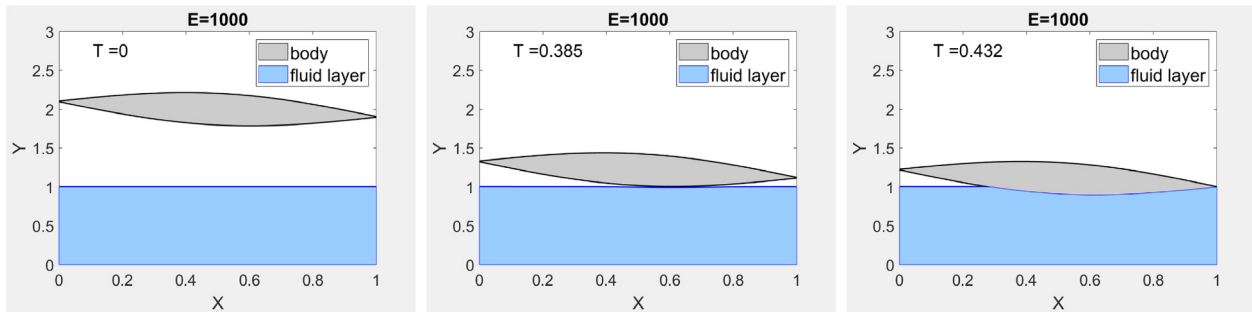

FIG. 4. The body motion and liquid layer reaction at three points in time for a density ratio $E = 1000$ (the air–water case) and an initially negative body angle, $\theta(0) = -0.2$. The layer shows no reaction to the body until it is very near. In the middle image, the intermediate regime 3 governs the dynamics near the contact point. This then progresses to wetting. In the rightmost image, we see a leveled off region (regime 1) at the leading edge and a wetted region (regime 2) at the trailing edge.

unity due to the Kutta requirement, we find from Eq. (8) the corresponding pressure response in the impact region is

$$p = \frac{1}{2}E\left(1 - \frac{1}{f^2}\right). \tag{12}$$

This remains $O(1)$ as contact with the liquid is approached.

IV. IMPACT SOLUTION IN THE $E \gg 1$ LIMIT

A natural question is how a large value of the density ratio E affects the conclusions of Sec. III. Expanding

$$F = \hat{F}_0(X, T) + E^{-1}\hat{F}_1(X, T) + \cdots, \tag{13}$$

where $E^{-1} \ll 1$, and denoting $\hat{A}(T) = H(1, T)$ as the trailing edge gap width, we arrive at the following hierarchical system at $O(1)$ and $O(E^{-1})$, respectively,

$$O(1) : \left[1 - \hat{F}_0^2\right](\hat{F}_0 - f)^2 = 0, \tag{14}$$

$$O(E^{-1}) : (\hat{F}_0^2 - 2\hat{F}_0\hat{F}_1)(\hat{F}_0 - f)^2 + 2(1 - \hat{F}_0^2)(\hat{F}_0 - f)F_1 = \hat{A}^2\hat{F}_0^2. \tag{15}$$
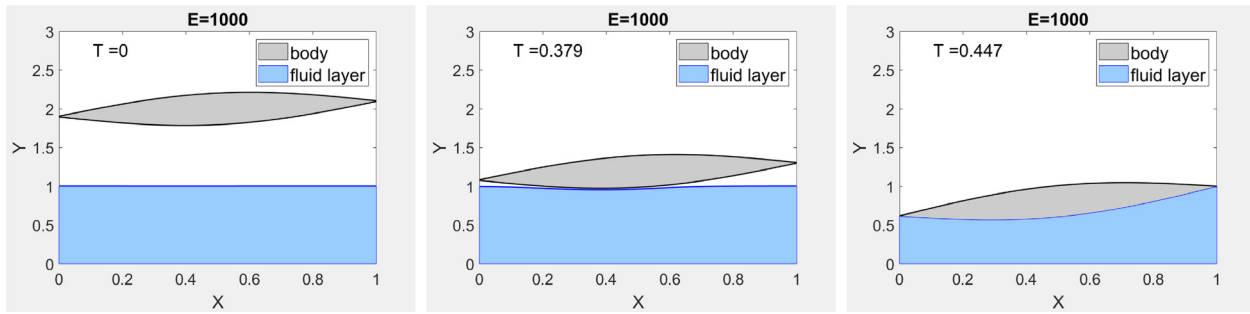
FIG. 5. The body motion and liquid layer reaction at three points in time for a density ratio $E = 1000$ (the air–water case) and an initially positive body angle, $\theta(0) = 0.2$. The layer shows no reaction to the body until it is very near. In the middle image, the intermediate regime 3 governs the dynamics near the contact point. This then progresses to wetting and eventually the full underbody is wetted in the rightmost image.

We see from Eq. (14) that either $\hat{F}_0 = 1$, the undisturbed height [note that $1/\alpha = \sqrt{E/(E-1)} \to 1$ as $E \to \infty$], or $\hat{F}_0 = f$ (impact). Analyzing Eq. (15) reveals three distinct asymptotic regimes which between them capture the range of behaviors of the layer leading up to impact. These have been termed "leveling off," "wetting," and "intermediate," and are discussed below in Subsecs. IV A, IV B, and IV C, respectively. All three regimes can be seen in Figs. 4 and 5 for $E = 1000$ (i.e., for air and water values).

A. Regime 1 (leveling off)

First we consider the case $\hat{F}_0 = 1 < f$, i.e., the body is relatively far from the layer and the layer is level to leading order (termed leveling off). We have

$$\hat{F}_1 = \frac{1}{2}\left(1 - \frac{\hat{A}^2}{(f-1)^2}\right), \tag{16}$$

hence

$$F = 1 + \frac{1}{2}E^{-1}\left(1 - \frac{\hat{A}^2}{(f-1)^2}\right) + \cdots. \tag{17}$$

It is then clear that for f close to 1 but $\hat{A}$ still $O(1)$, the second order term makes a contribution. This corresponds with our numerical results for large E (see Fig. 5 and Appendix), when the body is far from the layer, i.e., where the body shape is much below the trailing edge, we see a corresponding "dip" in the water (this intuition is given more careful treatment in Sec. IV C). The expansion in Eq. (17) agrees with Eq. (11), since in the case $\hat{A} = 0$ this is equal to the Taylor expansion of $(E/(E-1))^{1/2}$. The pressure response in this regime is

$$p = \frac{1}{2}\left(1 - \frac{\hat{A}^2}{(f-F)^2}\right), \tag{18}$$

here, corresponding to body–air interaction (Jolley and Smith, 2022), so pressure is $O(1)$ here. We see that as the trailing edge gap width $\hat{A} \to 0$, the pressure $p \to 1/2$ uniformly (a feature which is to be used later).

B. Regime 2 (wetting)

In this regime, we consider the second root of Eq. (14), for which the body is close to contact (but not yet in contact) with the layer, here

referred to as wetting. The rationale for the scales involved here is based on the squared factor $H(X, T)^2$ in Eq. (9) given that $H = f - F$ is small here. Thus, we can employ the expansion

$$F = f + E^{-1/2}\hat{A}F^* + \cdots \tag{19}$$

to obtain

$$F = f + E^{-1/2}\hat{A}\frac{f}{\sqrt{1-f^2}} + \cdots. \tag{20}$$

This applies both for $\hat{A} = O(1)$ and in the limit $\hat{A} \to 0$. For the pressure, we have Eq. (12), so $p = O(E)$ and the pressure is unchanged in the large E limit from the $E = O(1)$ case.

C. Regime 3 (intermediate)

In each of the above cases, a different regime is needed to explain the solution close to $f = 1$ when $\hat{A} = O(1)$ as both regimes 1 and 2 display singularities in this case. This corresponds to some portion of the body being close to the liquid layer rest height despite the trailing edge being still some distance away. We see from Fig. 3 that for smaller E, the layer tends to bend according to the body shape some time before impact, which prevents the body meeting the layer before the trailing edge has "caught up." However, for sufficiently large E, it is possible to have the body close to the layer (i.e., f close to 1) without requiring $\hat{A}$ to be small, see Figs. 4 and 5. The inherent balance here is between $E(F-1)H^2$ on the left-hand side of Eq. (9) and the $O(1)$ contribution on the right-hand side, with $(F-1)$ and H being comparably small. In this case, the expansions

$$F = 1 - E^{-1/3}\tilde{F} + \cdots \quad \text{and} \quad f = 1 - E^{-1/3}\tilde{f} + \cdots \tag{21}$$

are required, where we expect that $\tilde{F}$ is positive but $\tilde{f}$ can be either sign. Then we have, from Eq. (9), and recalling that $\hat{A}$ is the trailing gap width $H(1, T)$,

$$2\tilde{F}(\tilde{f} - \tilde{F})^2 = \hat{A}^2, \tag{22}$$

which is a cubic for $\tilde{F}$ in terms of $\tilde{f}$. It can be solved for $\tilde{f}$ to find

$$\tilde{f} = -\hat{A}\sqrt{\frac{1}{2\tilde{F}}} + \tilde{F}. \tag{23}$$

A plot of Eq. (23) is shown in Fig. 6. As can be seen in the figure, this matches with Eq. (17) as $\tilde{f} \to -\infty$ (i.e., body far away from the
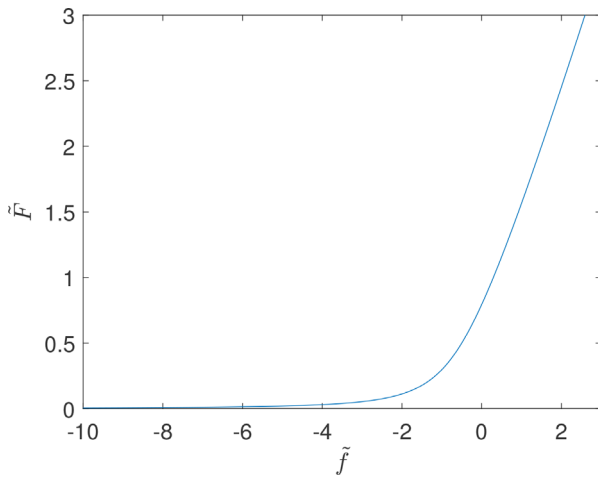
FIG. 6. A plot of Eq. (23), showing the leveling off behavior for large negative $\tilde{f}$ and the linear relationship for positive $\tilde{f}$, with $\hat{A} = 1$.

FIG. 7. Model for the post-impact analysis. This includes the moving contact point which is shown by a black cross (there, $X = X_0$). The latter is surrounded by an Euler region which is of short horizontal length scale but vertically spans the gap between the wall and the underbody and accommodates the turnover and jet root to the left of the contact point. The mass flux of liquid in the layer Q is 1 upstream of the contact point and less than 1 downstream. Strictly the wake is substantially longer than the body.

interface) and with Eq. (20) as solution $\tilde{f} \to +\infty$ (i.e., body pushing the layer below its rest height). The pressure in this regime is given by

$$p = -E^{2/3}\tilde{F}. \tag{24}$$

The body then continues to lower and this progresses to regime 2 (wetting). Again, there are two categories of outcome in general. The first, as shown in Fig. 4, is that the body impacts onto the layer with negative angle, creating two distinct regions, one wetted and one level (separated by an intermediate region). The second category is that the body impacts with positive angle, leading eventually to the whole underbody becoming wetted. In this second case, we expect the layer to flow over the top of the body; we do not model this outcome further in the present study. However, the former case leaves the possibility of further interesting dynamics including skimming, which is addressed in Sec. V.

V. POST-IMPACT MODEL

Returning now to assuming that the density ratio is order-one in general, suppose the body has impacted with the layer, creating a wetted region and a level region, as in Figs. 2 and 4. There is a stagnation point at (say) $X = X_0$ on the body surface where it meets the incoming liquid flow, which we refer to as the "contact point." As the body continues to lower, mass flux is lost at the trailing edge (thus a significant wake is created post-impact whereas none was present pre-impact). Since the incoming mass flux in the level region is unchanged, but the mass allowed to continue downstream into the wake is decreased, the mass must be accounted for in the vicinity of the contact point. We thus anticipate the formation of a jet along the underbody in $X < X_0$ to accommodate the lost mass of fluid from the layer and a pressure jump occurring at $X = X_0$. This is shown in Fig. 7. As discussed in Sec. I, the formation of a jet is typical in models of skimming, including Hicks and Smith (2011); Howison *et al.* (2004); Tuck and Dixon (1989).

Concerning the jet sketched in Fig. 7 (and appearing in Figs. 8–11 of results), its width at a given time remains spatially constant along the lower surface of the body because of the uniform pressure in
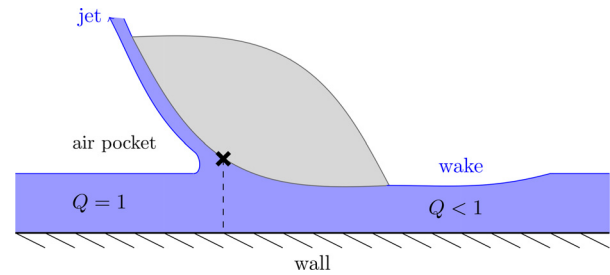
the air pocket but the width does vary with time due to mass conservation and the properties at the contact point. The jet instantaneously wets the whole lower surface ahead of the contact point. Notably, the jet then continues leftward and upward beyond the leading edge of the body because of the jet momentum; the same continuation applies throughout our subsequent results. A possibility is that the jet is then gradually turned rightward and upward by the oncoming air flow. The detailed travel of the jet beyond the body leading edge has no leading-order effect, however, on the dynamics of the body motion and the local three-way interplay between body, air, and liquid.

The presence of the jet creates an air pocket or bubble upstream of the contact point. As a consequence of the lack of vertical dependency in the problem, the air flow in the pocket is forced to be stagnant at leading order, so $p(X, T) = 1/2$ in this region, and $F(X, T) = 1/\alpha$. (Note that this is equal to the predicted values of pressure and liquid layer height under regime 1 as $\hat{A} \to 0$, as discussed in Sec. IV A.) The pressure in the wetted region downstream of the contact point where $X = X_0(T)$ is slightly altered from Eq. (12) due to the lowered trailing edge layer height, giving

$$p = \frac{1}{2}E\left(1 - \frac{F_1^2}{f(X, T)^2}\right), \tag{25}$$

where $F_1 = F(1, T) = f(1, T)$ is the trailing edge height, by use of Bernoulli's theorem and mass conservation. Thus, substituting this into Eq. (3), the motion is governed by

$$Mh_{TT} = \frac{1}{2}X_0 + \frac{1}{2}E\int_{X_0}^{1}1 - \left(\frac{f(1, T)}{f(X, T)}\right)^2 dX, \tag{26}$$

$$I\theta_{TT} = \frac{1}{4}X_0^2 - \frac{1}{2}\beta X_0 + \frac{1}{2}E\int_{X_0}^{1}(X - \beta)\left(1 - \left(\frac{f(1, T)}{f(X, T)}\right)^2\right) dX, \tag{27}$$

which can be solved numerically provided we can find the location of the contact point X_0.

Applying Bernoulli's theorem to the free surface along the inside of the pocket then yields that the velocity in the jet is $u = \alpha$ where $\alpha = \sqrt{1 - 1/E}$ by virtue of the results of Sec. III. Conservation of
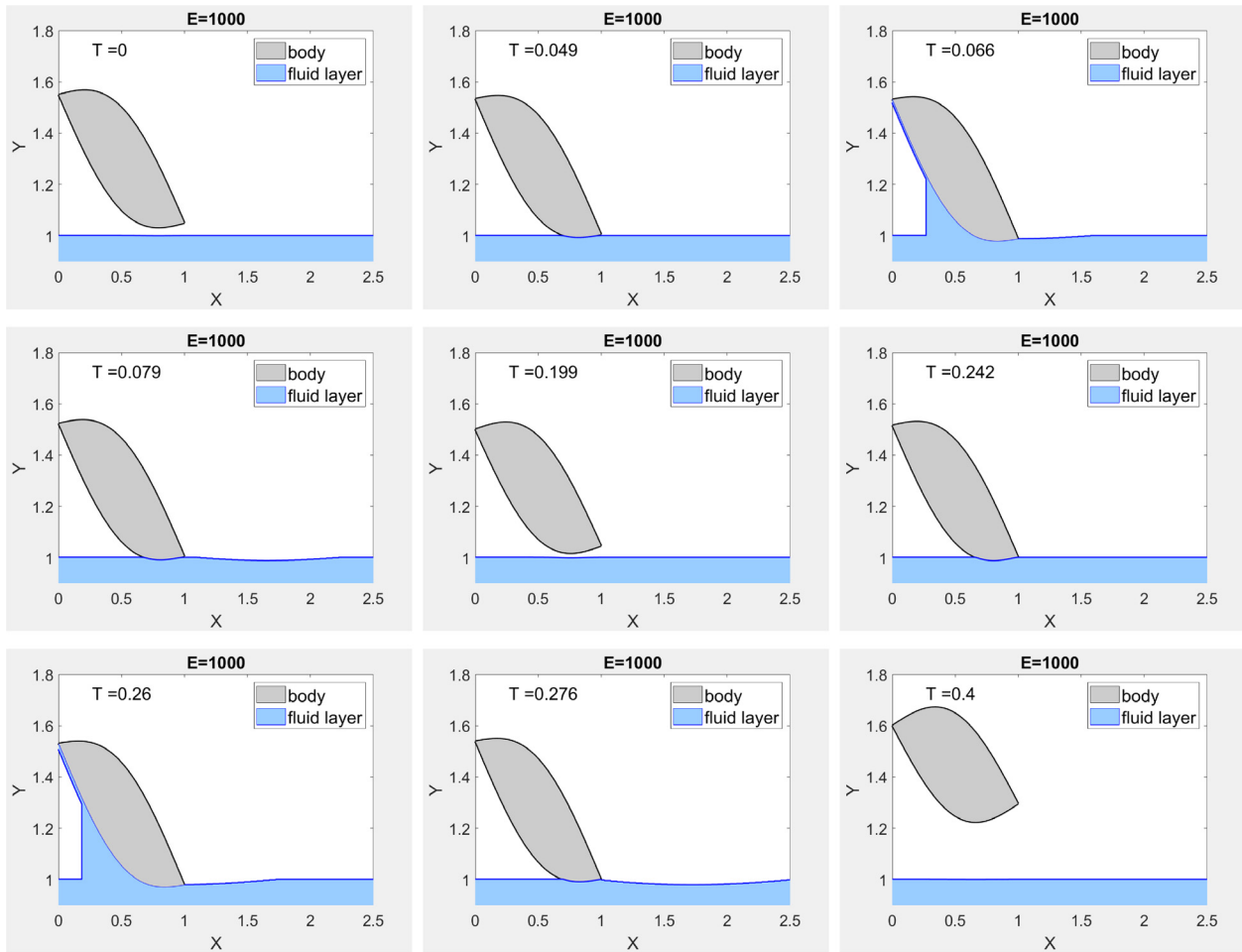
FIG. 8. Top left: The body in its initial position. Top middle: A first impact occurs. Top right: The jet and wake form (note this jet continues into the air ahead of the body). Middle left: The body lifts off and the wake travels downstream. Middle middle: The body rotates in the air. Middle right: The body returns for a second impact. Bottom left: A larger wake and jet form. Bottom middle: The body lifts off again and the wake travels downstream. Bottom right: The body flies away and does not return. More information about fly away phenomena can be found in [1]. The body has center of mass $\beta = 0.3$ and small moment of inertia to mass ratio $I/M = 0.01$.
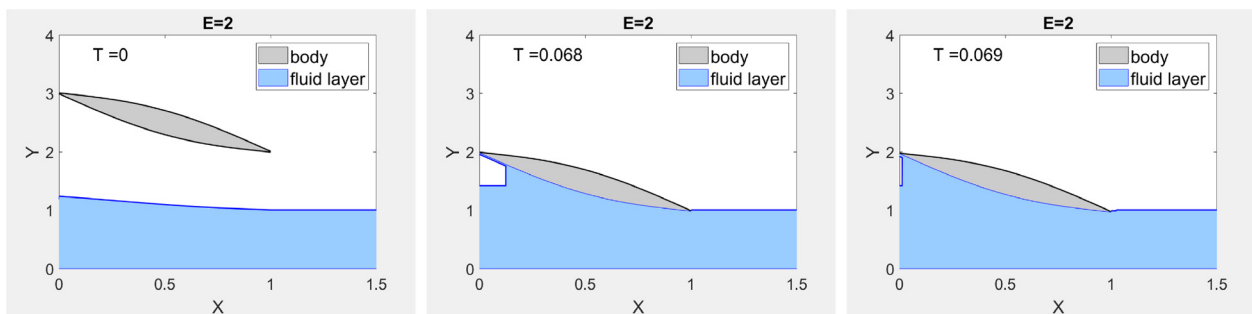

FIG. 9. A body impacting onto a layer with $E = 2$ and subsequently sinking. The left image shows the initial position of the body. It then impacts onto the layer, forming a jet (middle image). Note this jet continues into the air ahead of the body. The contact point then moves upstream until the underside of the body is fully wetted (right image).
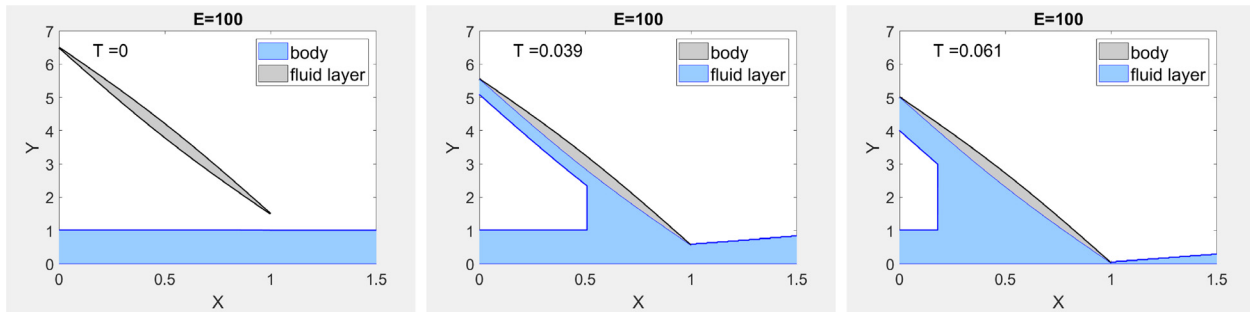
FIG. 10. A body impacting onto a layer with $E = 100$ and subsequently colliding with the wall at the trailing edge. The left image shows the initial position of the body. In the middle image, the body impacts onto the layer and a jet forms; this jet continues into the air ahead of the body. In the right image, the body collides with the wall.

mass between the incoming, outgoing and jet flows then yields the width of the jet as

$$\hat{h}_J = (1 - F_1)/\alpha. \tag{28}$$

Since all streamlines originally come from far upstream, we also have in the liquid

$$\frac{1}{2}u^2 + p/E = \frac{1}{2}. \tag{29}$$

Let the dividing streamline be given by $Y = \hat{h}(X, T)$, where $\hat{h}(X, T) = f(X, T)$ for $X > X_0$ (in other words, all flow below this streamline continues to the wetted region, and all that above the streamline is expelled through the jet). Then, we also have that

$$u\hat{h} = \text{independent of } X = F_1(T), \tag{30}$$

by conservation of mass, given that F_1 is the unknown height of the liquid at the trailing edge location. We note that the incident water height $F(X, T)$ remains unity upstream of the contact point $X = X_0(T)$. Conservation of momentum (comparing the momentum far upstream with that to the right of the contact point) yields

$$\frac{1}{2}(u_0^2 - u_L^2)\hat{h}_L = u_0^2\hat{h}_J + u_0^2\hat{h}_0 - u_L^2\hat{h}_L, \tag{31}$$

where u_L is the velocity following the pressure jump at the contact point and $\hat{h}_L = F(X_0, T) = f(X_0, T)$ is the corresponding height of the underbody there, while u_0 and $\hat{h}_0$ represent the velocity and layer height upstream of the contact point; thus, in our non-dimensionalization $u_0, \hat{h}_0$ are unity. In Eq. (31), the left-hand side represents the change in pressure across the jump while the right-hand side corresponds to the momentum lost from the system by the production of the jet. This is the criterion first derived in Tuck and Dixon (1989) and subsequently used in other models of stone skimming such as Hicks and Smith (2011), with allowance being made for the quasi-steady nature of the fluid flows here. Rearranging this using Eqs. (28) and (30), we have

$$u_L = \alpha\left(2\left(\frac{1}{\alpha\hat{h}_L}\right)^{1/2} - 1\right), \tag{32}$$

or equivalently, by Eq. (30),

$$F_1 = \alpha\left(2\left(\frac{\hat{h}_L}{\alpha}\right)^{1/2} - \hat{h}_L\right). \tag{33}$$

Since we know that $\hat{h}_L = f(X_0, T)$ and $F_1 = f(1, T)$ (since the body must be in contact at the trailing edge), we can find the contact point for a given body position using the relation

$$f(X_0, T) = \left[2 - f(1, T) + 2\sqrt{1 - f(1, T)}\right]/\alpha. \tag{34}$$

Knowing the contact point and pressure then allows the lift and moment to be found by Eqs. (26) and (27) and hence subsequent body positions, giving an algorithm for determining the motion of the body.

Numerical results reveal a number of possible behaviors. First, the body may skim, i.e., the additional lift from the liquid layer is sufficient to change the direction of motion of the body upward and it lifts off from the liquid layer. Its motion is then again governed by the pre-impact model as described in Secs. II and III. This allows repeat skims to occur, as shown in Fig. 8. (We remark in passing that, in the sense that the vertical scales are exaggerated compared with the horizontal, this figure and Figs. 9–13 are not to scale.) This figure demonstrates the body skimming twice and then flying away, for a density ratio $E = 1000$. The apparent vertical shock propagating in the liquid in the direction of wetting is smoothed out inside the moving Euler region. The shock is readily added into the figures based on the calculated region of wetting and the jet thickness. The flying away is due to the large Froude number and hence small gravitational effects compared with the lift force from the air—the effect of increasing gravity is discussed in Sec. VII. Other possible behaviors are sinking, where the body underside eventually becomes fully wetted (at which point our modeling ends) and "crashing," where the body collides with the wall before its underside is fully wetted. A sinking case is shown in Fig. 9 for $E = 2$, while crashing is addressed in Sec. VI.

A. Wake region

As the body impacts onto the layer, a wake forms downstream of the trailing edge. In the wake region, we have $p = 0$ and $u = 1$, and conservation of mass gives the equation

$$\varepsilon F_T + F_X = 0 \tag{35}$$

for the height of the liquid wake. Here, as a reminder, $\varepsilon = (L/\Delta)(\rho_a/\rho_B)^{1/2}$ is the unsteadiness parameter arising from the
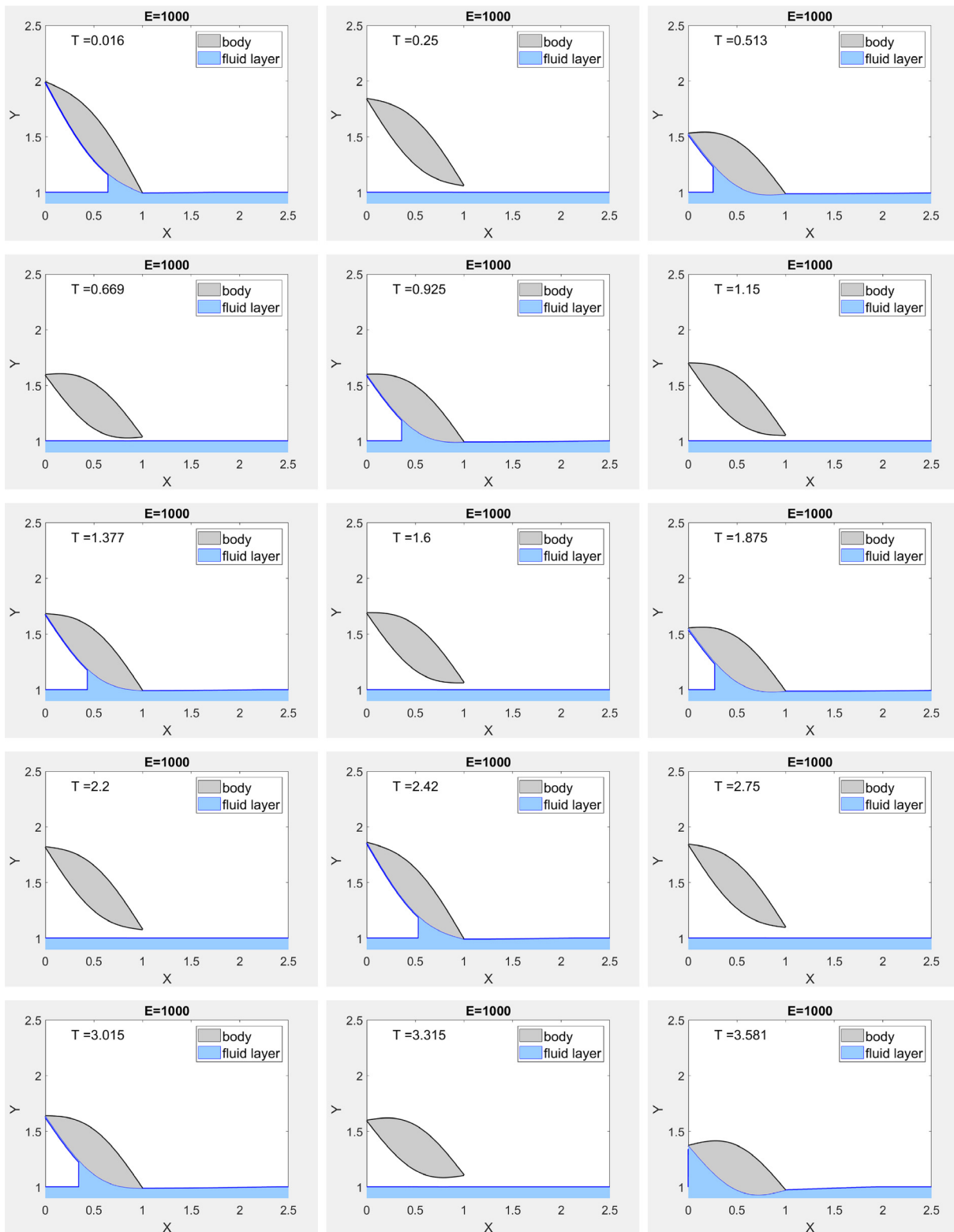
FIG. 11. Series of images depicting a series of seven skims followed by finally sinking in the bottom-most right image. Scaled gravity $\hat{g}$ was taken as 5.

choice of timescale, as in Eq. (1); provided the body is sufficiently heavier than the air this is a small parameter and hence unsteady terms were negligible until this point. Equation (35) is easily solved to yield

$$F(X, T) = F(1, T - \varepsilon X). \tag{36}$$

Hence, calculating the body motion also reveals the shape of its wake, in a sense. The wake can be seen downstream of the body during and after impact in Fig. 8. Notably, because of the factor epsilon in Eq. (35) the wake length is strictly much larger than the body length in this post-impact phase. The wake physics is simpler than in previous studies such as those by Hicks and Smith (2011) and Palmer and Smith (2022) because of the quasi-steadiness of the air and liquid flow over the body scale.

VI. IMPACT WITH WALL

In this section, we describe solutions where, following impact with the layer, the lift from the impact is not sufficient to change the downward direction of the body and hence it collides with the wall. This is shown in Fig. 10. The result is similar to the body–air crashes discussed in Jolley and Smith (2022) and Jolley et al. (2021).

A. First stage

In the post-contact regime (see Sec. V), we have that $p(X, T) = \frac{1}{2}$ to the left of the contact point and $p(X, T) = \frac{1}{2}E(1 - f(1, T)^2 / f(X, T)^2)$ to the right of the contact point. Suppose impact occurs at $X_1 > X_0$ at time T_1, and let $f(X, T) = O(T_1 - T)^n$ as $T \to T_1$ for $X = X_1 + O(T_1 - T)^{n/2}$ for some n to be determined. This leads to $n = 4/5$, the same time scaling as in the absence of water (Jolley and Smith, 2022; Jolley et al., 2021) since the dominant term in the pressure is still proportional to $1/f^2$.

B. Second stage

As in Jolley and Smith (2022) and Jolley et al. (2021), there is a second stage of the impact where the body velocity increases in the approach to the wall and flow unsteadiness asserts itself. Letting $T = T_1 + E^{-1/2}\tau t$ with the scale τ to be found, we have the following scalings in the inner region where $X = X_1 + \tau^{2/5}\xi$,

$$(h, \theta) = (h_1, \theta_1) + \tau^{4/5}(\tilde{h}, \tilde{\theta}), \quad p = E\tau^{-8/5}\tilde{p}, \quad u = \tau^{-4/5}\tilde{u}.$$

By conservation of mass and the Bernoulli equation, we then have

$$\tilde{u} = \frac{q(t)}{\phi(\xi, t)}, \quad \tilde{p} = -\frac{1}{2}\frac{q(t)^2}{\phi(\xi, t)^2}, \tag{37}$$

where $\phi(\xi, t) = \tau^{-4/5}f(X, T)$. In the outer region where X is of order unity, the momentum equation in the water is

$$uu_X + p_X = \varepsilon\tau^{-1}u_t, \tag{38}$$

where $\varepsilon = (L/\Delta)(\rho_a/\rho_b)^{1/2} = (L/\Delta)(\rho_w/\rho_b)^{1/2}E^{-1/2}$. Integrating this yields the "modified Bernoulli equation" in the same form as in the previously studied water-free case,

$$\frac{1}{2}u^2 + p = \begin{cases} \frac{1}{2}, & X < X_1, \\ \frac{1}{2} - \int_{-\infty}^{\infty} \tilde{u}_t \, d\xi, & X > X_1, \end{cases} \tag{39}$$

for $\tau = \varepsilon^{5/7}$. We thus see that the second stage dynamics are unchanged by the addition of a new fluid (the liquid) apart from the shorter timescale $E^{-1/2}\varepsilon^{5/7}$.

VII. EFFECT OF GRAVITY

The results in Fig. 8 display fly away, where after two skims the body lifts off to infinity, according to the fly away solutions described in Jolley and Smith (2022). This is a direct result of the high Froude number and hence lack of gravity in the problem. This is relevant to the aircraft icing application but of course is not usual in stone skimming games, for example. It is then of natural interest to investigate the effect of gravity on the body dynamics. Including gravity in Eq. (3) yields

$$Mh_{TT} = \int_0^1 p \, dX - M\frac{\rho_B}{\rho_a}\Delta\frac{1}{\text{Fr}^2} = \int_0^1 p \, dX - M\hat{g}. \tag{40}$$

Here, we have defined $\hat{g} = (\rho_B/\rho_a)\Delta/\text{Fr}^2$, the scaled gravity, where $\text{Fr} = U/\sqrt{gl}$ is the Froude number, U and l are the dimensional velocity and length scales and g is the gravitational acceleration constant. Considering $\hat{g}$ to be order one, gravity then makes a comparable contribution to pressure forces. Gravity then affects the body dynamics but is still negligible for the air and liquid layer flow. This is equivalent to the assumption that $(\rho_w/\rho_B) \ll \Delta/L$ (in words, the density ratio between the fluid and the body is much less than the aspect ratio of the body, which we have assumed is small). This is a weaker assumption than the previously assumed $(\rho_w/\rho_B) \ll (\Delta/L)^2$ for steady flow in the liquid, so valid under our current model, but again excludes the ice on water case. As may be expected, for sufficient gravity this disallows fly away and makes many repeated skims more achievable. The model results in Fig. 11 show a body skimming seven times before finally sinking.

VIII. CONCLUSION

There are three prime points to make from the present work. The first is that near-wall interaction between gas (e.g., air), liquid (e.g., water) and a freely moving body has been accommodated in the modeling. This can lead to impact of the body onto the liquid layer. Second, post-impact behavior has been included, showing air–water interactive effects on the skimming of the body consistent with a moving contact point within a moving Euler region. The third point here is that the skimming found is fully nonlinear and can produce complete sinking of the body or repeat skims, with multiple skims being seen in some results. The work is subject to several physical assumptions and simplifications of course but these are made on a rational basis.

Thus, the work in this paper has combined models of body–air interactions with a model body skimming on water (with air effects included) to describe the complete motion of a skimming body as it travels through the air and impacts onto water, repeatedly in some cases, as well as being able to describe other phenomena, such as sinking, as shown in Fig. 3. This has allowed the phenomenon of repeat skims to be fully captured, as demonstrated in Fig. 8 without gravity and Fig. 11 with gravity, the former being more relevant to aircraft icing, while the latter is more relevant to the more familiar "stone skimming" games. The result that repeat skims are possible

even in the gravity free case is surprising, and is a result of the complex and sensitive interactions between the particle and the air (the particle is pulled down purely by its interaction with the pressure forces in the air). Also surprising is the possibility of the particle being sent away from the wall entirely due to its interactions with the layer (fly away). This indicates that the presence of a layer of water could indeed be crucial to the behavior of an impinging particle. In the gravity case, the eventual sinking of the particle is often attributed to loss of horizontal momentum by drag forces, however in our model the particle loses no horizontal momentum at leading order but is still fated to sink eventually by the sensitivity of the system to its conditions. (To skim requires it to impact with specific conditions which are doomed to be violated eventually in any real system, or indeed simulation.)

The main findings, in short, are the cases of fly-away, skim, and sink responses in the free body motion when both air and liquid/water effects are admitted. These include multiple repeated skimmings as the body passes through the air, glances on the water, then rebounds and so on, followed by fly-away or by complete sinking onto the wall. Considerable wake displacements are also found to arise during each of the skims.

The model is applicable to a wide range of density ratios between the two fluids, but requires that the body is much denser than both. However, the case of an ice particle and a water layer can still be investigated by considering the limit of large density ratio between the two fluids. The adaptation of the model to accommodate bodies with density comparable to the liquid in the layer is still however the most obvious extension to the work in this paper. Other extensions include modeling multiple bodies rebounding, and investigating more closely other effects that may become relevant as the body is near or in the layer for a long period, since the model currently admits some solutions which do not appear physically realistic or are at least questionable, or perhaps are counter-intuitive, such as that described in the Appendix.

AUTHOR DECLARATIONS
Conflict of Interest

The authors have no conflicts to disclose.

Author Contributions

Ellen Mary Jolley: Formal analysis (equal); Investigation (equal); Project administration (lead); Software (lead); Writing – original draft (lead); Writing – review & editing (equal). **Frank T. Smith:** Formal analysis (equal); Investigation (equal); Supervision (lead); Writing – review & editing (equal).

DATA AVAILABILITY

Data sharing is not applicable to this article as no new data were created or analyzed in this study.

APPENDIX: SIMULTANEOUS IMPACT WITH BOTH LIQUID LAYER AND WALL

This appendix addresses the second impact solution to Eq. (9), specifically $F(X, T) = f(X, T) = 0$, where theoretically the body touches both the layer and the wall for the first time simultaneously. This can happen for body angles which are sufficiently positive for the leading edge to touch the wall while the trailing edge is still above the layer. This can be seen in Figs. 12 and 13 for two different E values. The layer being able to reach such a low level without any flow over the top of the body from upstream is counter-intuitive—we can think of this as a wave of increasing height building up in the Euler region just upstream of the leading edge, which may eventually break in reality. Since the pressure here is $p(X, T) = \frac{1}{2}(1 - H(1, T)^2/H(X, T)^2)$, this reproduces the asymptotic behavior for the other type of wall collision as described in Sec. VI. In reality here, as well as potential wave-breaking upstream of the leading edge, it is possible that other physical effects in the very thin layer of air between the body and the layer will become relevant.
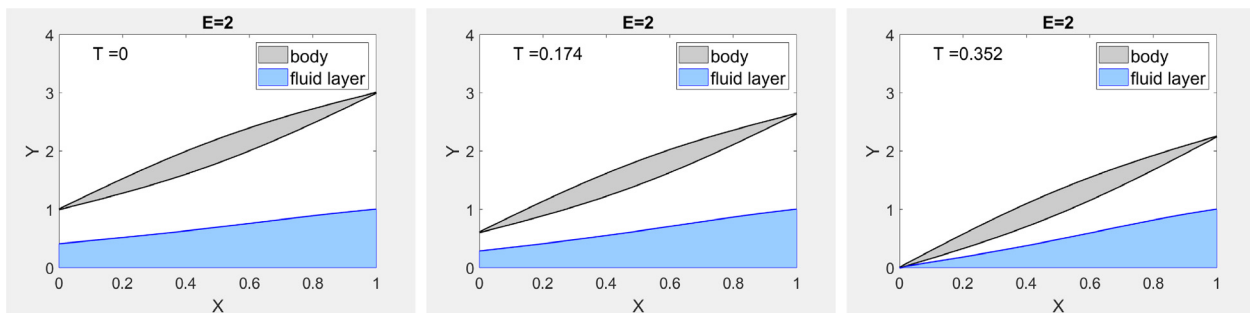

FIG. 12. The body motion and layer reaction at three points in time for a density ratio $E = 2$ and an initially positive body angle, $\theta(0) = 2$. The liquid layer reacts to the body motion even while it is still some distance away. Eventually, in the rightmost image, the body touches the wall before the trailing edge comes into contact—this is also the first time it touches the layer.
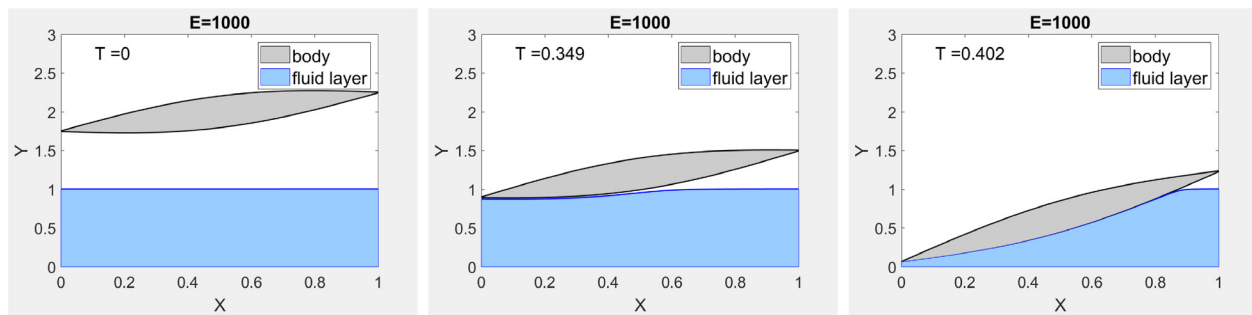
FIG. 13. The body motion and liquid layer reaction at three points in time for a density ratio $E = 1000$ and an initially positive body angle, $\theta(0) = 0.5$. The layer shows no reaction to the body until the body is very near. In the middle image, the intermediate regime 3 governs the dynamics near the contact point. This then progresses to wetting. Eventually, in the rightmost image, the body touches the wall before the trailing edge comes into contact—technically, in the model, this is the first time it touches the layer as well.

REFERENCES

Cointe, R. and Armand, J., "Hydrodynamic impact analysis of a cylinder," J. Offshore Mech. Arct. Eng. **109**(3), 237–243 (1987).

Gent, R. W., Dart, N. P., and Cansdale, J. T., "Aircraft icing," Philos. Trans. R. Soc. London, Ser. A **358**(1776), 2873–2911 (2000).

Hicks, P. D. and Smith, F. T., "Skimming impacts and rebounds on shallow liquid layers," Proc. Roy. Soc. A **467**(2127), 653–674 (2011).

Howison, S., Ockendon, J., and Oliver, J., "Oblique slamming, planing and skimming," J. Eng. Math. **48**, 321–337 (2004).

Howison, S. D., Ockendon, J. R., and Wilson, S. K., "Incompressible water-entry problems at small deadrise angles," J. Fluid Mech. **222**, 215–230 (1991).

Janjua, Z. A., Turnbull, B., Hibberd, S., and Choi, K.-S., "Mixed ice accretion on aircraft wings," Phys. Fluids **30**(2), 027101 (2018).

Jolley, E. M., Palmer, R. A., and Smith, F. T., "Particle movement in a boundary layer," J. Eng. Math. **128**, 6 (2021).

Jolley, E. M. and Smith, F. T., "A heavy body translating in a boundary layer: 'crash', 'fly away' and 'bouncing' responses," J. Fluid Mech. **936**, A37 (2022).

Jones, M. A. and Smith, F., "Fluid motion for car undertrays in ground effect," J. Eng. Math. **45**(3–4), 309–334 (2003).

Korobkin, A., "Impact of two bodies one of which is covered by a thin layer of liquid," J. Fluid Mech. **300**, 43–58 (1995).

Li, C., Wang, C., Wei, Y., Xia, W., and Zhang, C., "Hydrodynamic force and attitude angle characteristics of a spinning stone impacting a free surface," Phys. Fluids **33**(12), 123309 (2021).

Liu, K. and Smith, F. T., "Collisions, rebounds and skimming," Philos. Trans. R. Soc. A **372**(2020), 20130351 (2014).

Liu, K. and Smith, F., "A smoothly curved body skimming on shallow water," J. Eng. Math. **128**, 17 (2021).

Palmer, R. and Smith, F., "Skimming impacts and rebounds of smoothly shaped bodies on shallow liquid layers," J. Eng. Math. **124**, 41–73 (2020).

Palmer, R. A. and Smith, F. T., "Skimming impact of a thin heavy body on a shallow liquid layer," J. Fluid Mech. **940**, A6 (2022).

Palmer, R. A. and Smith, F. T., "The role of body shape and mass in skimming on water," Proc. R. Soc. A **479**(2269), 20220311 (2023).

Pinkstone, J., see https://www.telegraph.co.uk/news/2023/01/04/secret-skimming-stones-not-conventional-led-believe/ "Secret to skimming stones not as conventional as we've been led to believe" (Telegraph, 2023).

Purvis, R. and Smith, F., *Improving Aircraft Safety in Icing Conditions* (Springer, Germany, 2016), pp. 145–151.

Sample, I., see https://www.theguardian.com/science/2023/jan/04/potato-shaped-stones-are-better-for-skimming-say-experts for "Potato-shaped stones are best for skimming" (The Guardian, 2023).

Smith, F. T. and Ellis, A. S., "On interaction between falling bodies and the surrounding fluid," Mathematika **56**(1), 140–168 (2010).

Smith, F. T. and Servini, P., "Channel flow past a near-wall body," Q. J. Mech. Appl. Math. **72**(3), 359–385 (2019).

Tang, J., Zhao, K., Chen, H., and Cao, D., "Trajectory and attitude study of a skipping stone," Phys. Fluids **33**(4), 043316 (2021).

Tuck, E. O. and Dixon, A., "Surf-skimmer planing hydrodynamics," J. Fluid Mech. **205**, 581–592 (1989).

von Kármán, T., "The impact of seaplane floats during landing," Report No. NACA-TN-321 (NACA, 1929).

Wagner, H., "Über Stoß- und Gleitvorgänge an der Oberfläche von Flüssigkeiten," Z. Angew. Math. Mech. **12**(4), 193–215 (1932).